

Nonlinear electron heating by resonant shear Alfvén waves in the ionosphere

J. Y. Lu, R. Rankin, and R. Marchand

Department of Physics, University of Alberta, Edmonton, Alberta, Canada

V. T. Tikhonchuk

Centre Lasers Intenses et Applications, Université Bordeaux 1, Gradignan, France

Received 24 October 2004; revised 5 December 2004; accepted 14 December 2004; published 13 January 2005.

[1] Ionospheric electron heating by resonant standing shear Alfvén waves in Earth's magnetosphere is investigated. It is demonstrated that in field line resonances (FLRs), electron heating by Alfvén waves produces ionization and large changes in the ionospheric Pedersen conductivity. This leads to a strong feedback effect on the FLR amplitude, along with narrow localization in latitude. Analysis and computer simulations performed with a 2D finite element MHD code, indicate that the primary mechanisms responsible for variations in the electron temperature are ohmic heating by the electron component of the Pedersen current, and electron cooling due to ionization losses and collisions with neutrals. It is shown that electron heating can be quantitatively more important than direct collisional ionization by precipitating electrons. The latter can reduce dissipation losses by at most a factor of two. **Citation:** Lu, J. Y., R. Rankin, R. Marchand, and V. T. Tikhonchuk (2005), Nonlinear electron heating by resonant shear Alfvén waves in the ionosphere, *Geophys. Res. Lett.*, 32, L01106, doi:10.1029/2004GL021830.

1. Introduction

[2] Diffuse and discrete aurora are associated with electron precipitation in systems of field-aligned currents and parallel electric fields. Large scale field-aligned currents may have ionospheric latitudinal widths around 500 km, whereas discrete arcs may have km or sub-km scales [e.g., Stasiewicz and Potemra, 1998]. In discrete, temporally modulated auroral arcs, field-aligned currents produced by shear Alfvén waves must close through Pedersen currents in the ionosphere. If the conductivity of the ionosphere is low, shear Alfvén waves will be strongly damped, and thus it is important to consider factors affecting the conductivity. Ionospheric feedback [e.g., Lysak and Song, 2002], involving ionization by precipitating electrons, is one process by which conductivity enhancements may allow shear Alfvén waves to sustain or grow in regions of initially low conductivity. However, it can be shown that in arcs associated with long period field line resonances (FLRs) [e.g., Lu et al., 2003], this process is not very effective [Prakash et al., 2003].

[3] Lysak and Song [2002] recently calculated Pedersen conductivity modulations resulting from ionospheric over-reflection of Alfvén wave energy. Streltsov and Foster [2004] considered electrons precipitating through parallel

currents, finding that the dependency of the Pedersen conductivity on the parallel current can lead to the ionospheric feedback instability within the Alfvénic resonator. However, as pointed out by Prakash et al. [2003], the modulation of conductance by precipitating energetic electrons is important in FLRs only at a very low background conductance, and in the frequency range 0.1–1 Hz. In order to be effective, precipitating electrons in low frequency (mHz) FLRs must have high precipitation energies (several hundreds of eV) to initiate Pedersen conductivity enhancements. Specifically, precipitating electrons affect only the local conductivity over one half of a wave period, and cannot reduce losses by j_{\perp} by more than a factor of two [Prakash et al., 2003].

[4] The conductivity of magnetospheric field lines supporting shear Alfvén waves is also important in the evolution of FLRs. For example, Tikhonchuk and Rankin [2002] studied a mechanism for forming parallel electric fields that is based on a nonlocal electron kinetic response to standing shear Alfvén waves on stretched magnetic fields. They demonstrated that the frequency dependent conductivity of auroral field lines becomes particularly small, especially inside density cavities. Their nonlocal conductivity mechanism was subsequently extended to higher frequency waves trapped in the ionospheric Alfvén resonator [Lysak and Song, 2003]. It is clear from these that proper treatment of wave and ionospheric conductivities is necessary to understand magnetosphere-ionosphere coupling involving Alfvén waves.

[5] In this paper, we analyse heating and ionization of ionospheric plasma by standing shear Alfvén waves. A new nonlinear electron heating mechanism in the ionosphere is presented. By using the temperature dependent plasma conductivity in a 2D finite element MHD model of FLRs, we demonstrate how this leads to an enhancement of the ionospheric Pedersen conductivity by field-aligned currents, and address how ionospheric feedback affects FLR dynamics.

2. Analysis of Shear Alfvén Wave Ohmic Heating in the Ionosphere

[6] Field-aligned currents play an important role in magnetosphere-ionosphere coupling. In particular, magnetospheric field-aligned currents are closed by Pedersen and Hall currents in the ionosphere. Here, we shall neglect the Hall current for simplicity. To orient our analysis, consider a typical wave field-aligned current $j_{\parallel} = 10 \mu\text{A}/\text{m}^2$ that exists over a characteristic ionospheric width of $a = 10$ km. The ionospheric current can be estimated from the equation for

current continuity: $j_{\perp} = j_{\parallel}/h = 5 \mu\text{A}/\text{m}^2$, assuming an ionospheric layer of height $h = 20 \text{ km}$. For a typical Pederson conductivity of $\sigma_{pi} = 10^{-4} \text{ S/m}$, the associated ionospheric electric field strength corresponds to $E_{\perp} = j_{\perp}/\sigma_{pi} = 0.05 \text{ V/m}$. For reference, this provides a perpendicular potential drop of about 0.5 kV at the half-period of the shear Alfvén wave.

[7] Consider a reference system in which neutrals are at rest. The energy balance equations at the ionosphere are then governed by [Cravens, 1997]

$$\begin{aligned} \frac{3}{2}n_e \frac{dT_e}{dt} + n_e T_e \nabla \cdot \mathbf{u}_e + \nabla \cdot \mathbf{q}_e &= W_{Te} - \nu_e \frac{2m_e}{m_n} n_e (T_e - T_n), \\ \frac{3}{2}n_i \frac{dT_i}{dt} + n_i T_i \nabla \cdot \mathbf{u}_i + \nabla \cdot \mathbf{q}_i &= W_{Ti} - \nu_i n_i (T_i - T_n), \\ \frac{3}{2}n_n \frac{dT_n}{dt} + \nabla \cdot \mathbf{q}_n &= \nu_e \frac{2m_e}{m_n} n_e (T_e - T_n) + \nu_i n_i (T_i - T_n), \end{aligned} \quad (1)$$

where $W_{Te,i}$ is the energy released in the corresponding charge, $\nu_{e,i}$ is the collision frequency with neutrals, $\mathbf{u}_{e,i}$ is the velocity of heat convection, and \mathbf{q} is the conductive heat flux defined by $\mathbf{q} = -n\nu\lambda\nabla T$ (here λ is the mean free path of the corresponding particle).

[8] In the ionosphere, where the neutral density (and thus the electron-neutral and ion-neutral collision frequencies) is high, local collisional energy transfer becomes more important than convective or conductive heat transport in the energy balance relation: The heating power $W_{Ti} = E_{\perp}j_{\perp} = 2.5 \times 10^{-7} \text{ W/m}^3$ is released predominantly in the ion component because it is the ions that carry the Pedersen current. For a typical ion density $n_i = 2.5 \times 10^4 \text{ cm}^{-3}$, one finds a heating rate of $10^{-17} \text{ W} = 100 \text{ eV/s}$ per ion. However, this ion heating does not result in a rapid temperature increase because the energy exchange time between ions and neutrals is very fast ($1/\nu_i = 0.01 \text{ s}$). Therefore, ions and neutrals remain in approximate equilibrium and the heating power per atom will be about 10^{-5} eV/s for neutrals with density $n_n = 10^{11} \text{ cm}^{-3}$. This heating rate is mainly balanced by heat conductivity, i.e., $W_{Ti} \approx n_n T_n \nu_n (\lambda_n/a)^2$, which translates to a neutral temperature $T_n \sim 0.1 \text{ eV}$, which can be ignored. The corresponding heating time is about 3 hrs, which is significantly longer than the characteristic ionospheric life time of ionized particles.

[9] Heating of electrons, rather than ions, represents the dominant energy exchange mechanism. To see this, note that the electron current is defined by,

$$j_{\perp e} = \sigma_{pe} E_{\perp} = j_{\perp} \frac{\nu_e / \Omega_e}{\nu_i / \Omega_i}. \quad (2)$$

For an electron conductivity of $\sigma_{pe} = 5 \times 10^{-7} \text{ S/m}$, we find $j_{\perp e} = 0.005 j_{\perp}$, and correspondingly, the heating power is roughly $W_{Te} = 0.005 W_{Ti}$, i.e., about 10^{-9} W/m^3 or 0.2 eV/s per electron. Although this is much less than for ions, the electron losses are also much smaller. There are two processes by which an electron can lose energy: through e-n collisions with energy exchange rate $2\nu_e m_e / m_n$, and by electron heat conductivity along magnetic field lines (electrons are strongly magnetized and their heat conductivity is primarily along the field lines). The energy exchange time is roughly 1 s, i.e., shorter than the heat conductivity time $1/\nu_e (h/\lambda_e)^2$ of around 100 s. Correspond-

ingly, the electron temperature will be defined by a balance between heating and cooling processes:

$$\Delta T_e = (W_{Te}/n_e \nu_e)(m_n/m_e), \quad (3)$$

which gives roughly 0.2 eV for our chosen parameters. This temperature increase is comparable to the initial electron temperature, and therefore this example defines a reasonable boundary between linear and nonlinear ionospheric responses: the temperature increases in proportion to the square of the current and, for a parallel current of $20 \mu\text{A}/\text{m}^2$, the electron temperature will be approximately 1 eV. This is a large increase in temperature comparable to the ionization potential $\varphi = 8 \text{ eV}$ of oxygen and nitrogen, and thus it will cause additional ionization. Correspondingly, the electron density will increase, bring about a larger Pedersen conductivity, and thus reduce the ionospheric electric field and dissipation.

3. Nonlinear Electron Heating Mechanism

[10] The electron production in the ionosphere is derived from photoionization and/or electron impact ionization and from chemistry, while electron losses are mainly due to ion-neutral reactions and electron-ion recombination. The ionization in the E-layer is produced by inelastic collisions of heated electrons and external sources such as cosmic rays. If chemical production and losses are ignored, ionization is balanced by recombination, as defined by the electron density continuity equation

$$\partial_t n_e = S + \nu_{\text{ioniz}} n_e - R n_e^2, \quad (4)$$

where S is the external source, ν_{ioniz} is the ionization rate given by $\nu_{\text{ioniz}} = 0.1 \nu_e \exp(-\varphi/T_e)$, and $R = 10^{-13} \text{ m}^3/\text{s}$ is the constant of recombination, which gives an effective recombination rate of 0.0025 s^{-1} ($\nu_{\text{rec}} = R n_e$).

[11] In the stationary approximation, from the balance between collisional ionization and recombination, one can estimate the electron temperature using

$$T_* = \varphi / \ln(0.1 \nu_e / \nu_{\text{rec}}). \quad (5)$$

For $\varphi = 8 \text{ eV}$, $\nu_{\text{rec}} = 0.0025 \text{ s}^{-1}$, and $\nu_e = 10^4 \text{ s}^{-1}$, this is 0.9 eV. The rise in electron temperature in this regime is a very weak function of the electron density.

[12] In the stationary approximation, and neglecting diffusion and convection losses, equations (1) and (4) reduce to the following system for the electron density and temperature

$$n_e^2 - n_{e0}^2 = \frac{\nu_{\text{ioniz}} n_e}{R}, \quad (6)$$

$$\frac{j_{\perp}^2}{\sigma_{p0}} = \frac{n_e^2}{n_{e0}} \frac{\nu_i}{1 + \nu_i^2 / \Omega_i^2} (T_e - T_n), \quad (7)$$

where $n_{e0} = \sqrt{S/R}$ is the unperturbed electron density and in the energy balance equation we used $m_n = 2m_i$. Equation (7) defines the critical Pedersen current

$$j_c = \sqrt{\sigma_{p0} n_{e0} \frac{\nu_i}{1 + \nu_i^2 / \Omega_i^2} T_*} = \sigma_{p0} B_0 \nu_{i*}, \quad (8)$$

which is needed to enter in the nonlinear regime (see the explanation in next paragraph). Here, $\nu_{i*} = \sqrt{T_*/m_i}$ is the

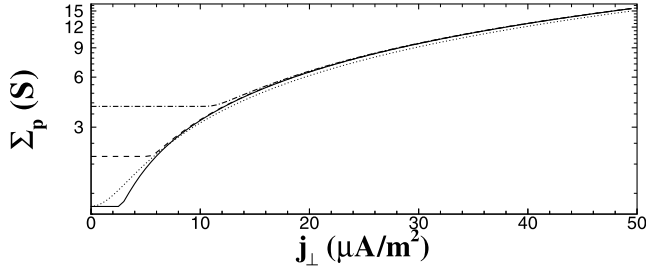


Figure 1. Pedersen conductivity as a function of ionospheric current for $\Sigma_{P0} = 1$ S (solid), 2 S (dashed), and 4 S (dash-dot). Here we also include a comparison between analytic approximation $\Sigma_P = \Sigma_{P0} \sqrt{1 + (j_{\perp}/J_c)^2}$ (dotted) and the numerical result of directly solving equations (6) and (7) for $\Sigma_{P0} = 1$ S. In the analytic solution, $J_c = 0.033$ A/m. The two results are asymptotically the same in the nonlinear regime.

characteristic ion velocity and B_0 is the strength of Earth's magnetic field. Integration of equation (8) over the height of the ionosphere defines the height-integrated critical current $J_c = \Sigma_{P0} B_0 \sqrt{T^*/m_i}$.

[13] There are two limits in the solution of equations (6) and (7). In the linear regime, $j_{\perp} < j_c$, equation (7) defines the rise in electron temperature, $T_e = T_n + T^*(j_{\perp}/j_c)^2$, which is smaller than T^* . In this limit, the ionization frequency in equation (6) is negligible and we may assume $n_e \approx n_{e0}$. At the critical current, j_{\perp} satisfies equation (7) for $n_e = n_{e0}$ and then we have $T_e = T^*$. In the nonlinear regime, the ionization term in equation (6) becomes dominant, and leads to saturation of T_e at the value T^* . In this limit, equation (7) defines the electron density: $n_e \approx n_{e0} |j_{\perp}/j_c|$. Therefore, the electron density can be reasonably approximated by

$$n_e = n_{e0} \sqrt{1 + (j_{\perp}/j_c)^2}, \quad (9)$$

which means that in the nonlinear regime, the electron temperature is clamped at a level below 1 eV by the ionization/recombination process and the electron density increases in proportion to j_{\perp} . The dependence of Joule heating on j_{\perp} will change from a quadratic function in the linear regime to a linear function because the conductivity increases with j_{\perp} . This corresponds to a nonlinear wave damping that is inversely proportional to the parallel current. Using the above interpolation formula for the electron density, the Joule heating rate can be written as

$$W_T = \frac{j_{\perp}^2}{\sigma_{P0}} \frac{1}{\sqrt{1 + (j_{\perp}/j_c)^2}} \quad (10)$$

[14] Equations (9) and (10) can also be written in terms of height-integrated quantities, respectively

$$N_e = N_{e0} \sqrt{1 + \left(\frac{J_{\perp}}{J_c}\right)^2}, \quad Q = \frac{J_{\perp}^2}{\Sigma_{P0}} \frac{1}{\sqrt{1 + (J_{\perp}/J_c)^2}} \quad (11)$$

where the height-integrated Pedersen current follows the current continuity equation: $dJ_{\perp}/dx = -j_{\parallel}$. Therefore, the nonlinear regime does not depend on the ionospheric thickness h , but only on the total parallel current $\int j_{\parallel} dx \sim j_{\parallel} a$. For $j_{\parallel} = 10 \mu\text{A}/\text{m}^2$ and $h = 10$ km, we have $J_{\perp} = 0.1$ A/m, about 3 times of the critical value. It can be deduced that

nonlinear heating is much more efficient than collisional ionization by precipitating electrons. As mentioned above, the latter only affects the local conductivity during half of the wave period, and thus it cannot reduce the losses by j_{\perp} by more than a factor of two.

[15] Figure 1 shows the dependence of the Pedersen conductivity on the magnitude of the ionospheric current. It can be seen that the conductivity increases significantly with j_{\perp} . The numerical results in Figure 1, which are obtained by directly solving equations (6) and (7), for $\Sigma_{P0} = 1, 2,$ and 4 S, respectively, show the obvious critical current that is required for electron Ohmic heating to be effective. It can also be seen that the critical current increases in proportion to the initial conductivity in the ionosphere. When the field-aligned current exceeds the critical current, the nonlinear heating regime comes into play. This regime depends on the ionospheric current, and not on the initial conductivity. Figure 1 also shows a comparison between the analytic approximation ($\Sigma_P = \Sigma_{P0} \sqrt{1 + (j_{\perp}/J_c)^2}$) and the numerical result of equations (6) and (7). The two results provide excellent agreement in the nonlinear regime.

4. Numerical Results

[16] Here, we combine our theory of Ohmic heating with the FLR numerical model described by *Lu et al.* [2003]. By way of illustration, we drive a magnetic perturbation at the equator, with a frequency matching the Alfvén wave eigenfrequency of 8.6 mHz on the dipolar magnetic shell $L = 8$. The height of the ionosphere is assumed to be 10 km, and the ionospheric boundary is placed at an altitude of 80 km. The finite element model TOPO [*Marchand and Simard, 1997*] is used to solve the 2D reduced MHD equations [*Lu et al., 2003*] and 1D equations (6) and (7) for ionospheric electrons. The model for FLRs takes into account the variation of temperature and density along and across the magnetic field lines, along with wave dispersive effects. In the case of a dipolar field at $L = 8$, dispersive effects can be neglected. Then, the limiting perpendicular scale of the FLR is determined by losses and the associated Pedersen conductivity.

[17] Figure 2 shows the wave azimuthal magnetic field perturbation (B_{ϕ}), parallel current (j_{\parallel}), perpendicular electric field (E_{\perp}), and perpendicular current (j_{\perp}) at the ionosphere. The results correspond to $\Sigma_P = \infty$ (dotted), fixed conductivity $\Sigma_P = 2.0$ S (dashed), and time-dependent conductivity (solid) associated with nonlinear electron heating (starting from an initial conductivity $\Sigma_{P0} = 2.0$ S). For the perfect conductivity case, the magnetic perturbation and parallel current are both very large by $t = 20$ periods, whereas the perpendicular electric field is zero. Fixed finite ionospheric conductivity reduces the level of the wave magnetic field and currents: B_{ϕ} at the ionosphere decreases from 522 nT to 167 nT; j_{\parallel} drops from 29 to 3 $\mu\text{A}/\text{m}^2$, and j_{\perp} drops from 38 to 12 $\mu\text{A}/\text{m}^2$. Correspondingly, finite conductivity leads to an increase in E_{\perp} from zero to 66 mV/m.

[18] When nonlinear heating is turned on, the Pedersen conductivity increases, and the ionospheric electric field and wave dissipation are reduced in comparison to the case with fixed conductivity. In Figure 2, the amplitude of the azimuthal magnetic field is enhanced from 167 nT in the fixed ($\Sigma_P = 2$ S) conductivity case, to 309 nT in the nonlinear heating case. The field-aligned and ionospheric currents

increase from 3 to 10 $\mu\text{A}/\text{m}^2$, and from 12 to 22 $\mu\text{A}/\text{m}^2$, respectively, while the perpendicular electric field is reduced from 66 mV/m to 32 mV/m. Note that the Pedersen conductivity increases by about a factor of four ($\Sigma_P = 7.7$ S) in saturating at around 15 periods. For completeness, Figure 3 shows the profiles of the saturated j_{\parallel} and E_{\perp} along the magnetic field line ($L = 8$) for an initial ambient conductivity of $\Sigma_{P0} = 2$ S. It can be seen that j_{\parallel} and E_{\perp} have characteristic maxima at the ionospheric ends, while E_{\perp} has a minimum at the equator.

[19] Our numerical results indicate that the saturated value of Σ_P in the nonlinear regime has no significant dependence on Σ_{P0} . This can be understood from Figure 1, which shows that Σ_P does not depend on Σ_{P0} under the condition that the ionospheric current is constant. We also find that the saturated parallel current and electric field are almost identical, irrespective of whether we start from $\Sigma_{P0} = 1$ S, 2 S or 4 S. This indicates that ionospheric feedback is very effective at small initial Pedersen conductivities (<2 S). The increase of Σ_P by nonlinear heating, as well as the corresponding enhancement of wave fields and currents, does, however, depend on the amplitude of the driver for shear Alfvén waves, which must create field-aligned currents that exceed the critical current defined by our analysis.

5. Conclusions

[20] We have analysed heating of the ionosphere by long period standing shear Alfvén waves, and demonstrated that

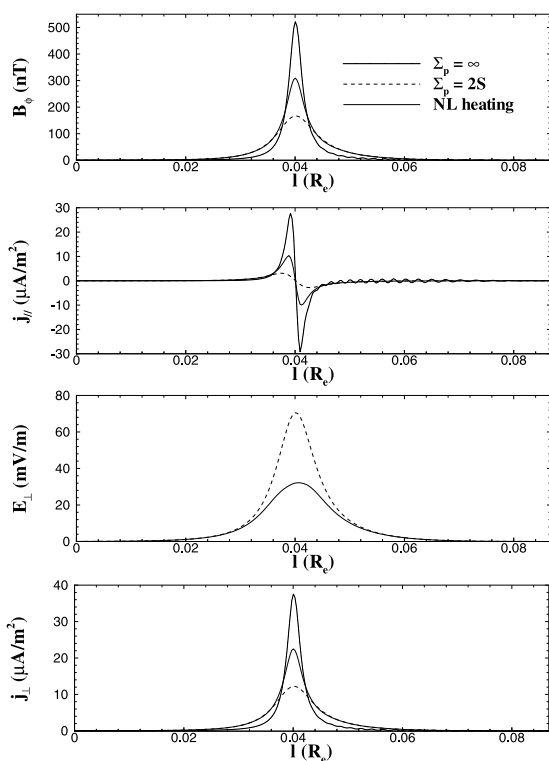


Figure 2. Comparison of the wave fields between perfect conductivity (dotted), a fixed conductivity $\Sigma_P = 2$ S (dashed) and a nonlinear heating with $\Sigma_{P0} = 2$ S (solid) at $t = 20$ periods. B_{ϕ} , j_{\parallel} , E_{\perp} , and j_{\perp} at the ionosphere are shown. l corresponds to the distance in Earth radius across field lines at the ionospheric boundary.

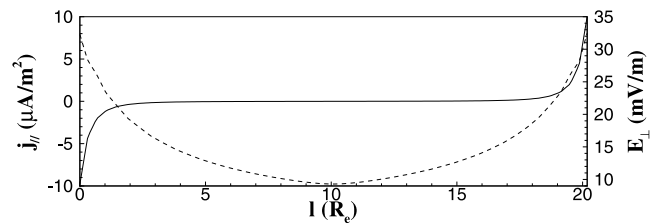


Figure 3. Profiles of j_{\parallel} (solid) and E_{\perp} (dashed) along the magnetic field line around shell $L = 8$. l corresponds to the distance in Earth radius along the field line.

the electron temperature is defined by a balance between Ohmic heating of the electron component of the Pedersen current, and electron cooling due to ionization losses and collisions with neutrals. The electron Pedersen current is small in comparison to the corresponding ion component, but experiences significantly lower losses. Provided parallel currents exceed a critical value defined by our analysis, we show that the resulting electron temperature increase, leads to significant ionization and large changes in the Pedersen conductivity.

[21] A self-consistent 2D finite element MHD model has been used to study the effect of nonlinear electron heating on magnetospheric FLRs. It is shown that for realistic parameters of FLRs, heated electrons produce ionization that can change the Pedersen conductivity by a large factor. An important feature of our nonlinear heating mechanism is that it does not require high precipitation energies of electrons to initiate Pedersen conductivity enhancements. In particular, in the case of low frequency (mHz periods) FLRs, nonlinear electron heating is found to be quantitatively more important than ionization produced by precipitating electrons. It is also more effective for smaller ambient conductivities (<2 S), suggesting, perhaps, that discrete arcs associated with latitudinally narrow FLRs, may have their birth in regions of low background conductivity.

References

- Cravens, T. E. (1997), *Physics of Solar System Plasmas*, Cambridge Univ. Press, New York.
- Lu, J. Y., R. Rankin, R. Marchand, V. T. Tikhonchuk, and J. Wanliss (2003), Finite element modelling of nonlinear dispersive field line resonances, *J. Geophys. Res.*, *108*(A11), 1394, doi:10.1029/2003JA010035.
- Lysak, R. L., and Y. Song (2002), Energetics of the ionospheric feedback interaction, *J. Geophys. Res.*, *107*(A8), 1160, doi:10.1029/2001JA000308.
- Lysak, R. L., and Y. Song (2003), Nonlocal kinetic theory of Alfvén waves on dipolar field lines, *J. Geophys. Res.*, *108*(A8), 1327, doi:10.1029/2003JA009859.
- Marchand, R., and M. Simard (1997), Finite element modelling of Tdew edge and divertor with $\mathbf{E} \times \mathbf{B}$ drifts, *Nucl. Fusion*, *37*, 1629–1639.
- Prakash, K., R. Rankin, and V. T. Tikhonchuk (2003), Precipitation and nonlinear effects in geomagnetic field line resonances, *J. Geophys. Res.*, *108*(A4), 8014, doi:10.1029/2002JA009383.
- Stasiewicz, K., and T. Potemra (1998), Multiscale current structures observed by Freja, *J. Geophys. Res.*, *103*, 4315–4326.
- Streltsov, A., and J. C. Foster (2004), Electrodynamics of the magnetosphere-ionosphere coupling in the nightside subauroral zone, *Phys. Plasmas*, *11*, 1260–1267, doi:10.1063/1.1647139.
- Tikhonchuk, V. T., and R. Rankin (2002), Parallel potential driven by a kinetic Alfvén wave on geomagnetic field lines, *J. Geophys. Res.*, *107*(A7), 1104, doi:10.1029/2001JA000231.

J. Y. Lu, R. Marchand, and R. Rankin, Department of Physics, University of Alberta, Edmonton, AB, Canada T6G 2J1. (jlu@space.ualberta.ca)
V. T. Tikhonchuk, Centre Lasers Intensites et Applications, Universite Bordeaux 1, F-33175 Gradignan cedex, France. (tikhon@celia.u-bordeaux1.fr)